Rietveld Structure Refinements of Calcium Hydroxylapatite Containing Magnesium

A. Bigi, G. Falini, E. Foresti, M. Gazzano, A. Ripamonti and N. Roveri

Dipartimento di Chimica 'G. Ciamician' and Centro di Studio per la Fisica delle Macromolecole, Università degli Studi di Bologna, Via Selmi No. 2, I-40126 Bologna, Italy

Abstract

The crystal structures of four hydroxylapatite (HA) samples prepared from solutions in the presence of 10, 15, 25 and 30 Mg-atom-% have been investigated by X-ray powder pattern fitting. The total magnesium content of the solid samples, as determined by chemical analysis, was 4.9, 14.1, 20.4 and 30.6 Mg-atom-%, respectively. Rietveld analysis was performed using the computer program *PREFIN* implemented with routines which allow the refinements of the average crystallite sizes. Different refinement procedures were carried out in order to evaluate the effect of the amorphous and background profiles on the occupancy factor data. For comparison, magnesium-free hydroxylapatite was refined with the same strategies. The results of the different approaches indicate that the degree of magnesium substitution for calcium in the HA structure can be at most ~ 10 atom-%. Magnesium substitutes calcium preferentially at the $6(h)$ site. The broadening of the diffraction peaks increases on increasing the total magnesium content in the solid phase, which is always significantly higher than the amount incorporated into the HA structure. The excess is probably located in the amorphous phase and/or on the crystallite surface.

1. Introduction

Numerous cations can substitute for calcium in the structure of hydroxylapatite, $Ca_{10}(PO_4)_6(OH)_2$, inducing modifications of the crystallinity, morphology, lattice parameters and stability of the apatite structure.

The incorporation of cations other than Ca^{2+} into the HA structure generally provokes a decrease in its stability (Heijligers, Driessens & Verbeck, 1979; Le Geros & Le Geros, 1984; Baravelli, Bigi, Foresti, Ripamonti & Roveri, 1984; Bigi, Gazzano, Ripamonti, Foresti & Roveri, 1986; Bigi *et al.*, 1991). The destabilizing effect of some ions, such as Mg^{2+}, Mn^{2+}, Fe^{2+}, Co^{2+} and Ni^{2+}, is so evident that they inhibit the synthesis of HA, promoting the formation of β-tricalcium phosphate [β-TCP (Le Geros, Taheri, Quirolgico & Le Geros, 1980; Nancollas, 1982)]. Even at low concentration Mg^{2+}, Ni^{2+}, Fe^{2+} or Co^{2+} severely strain the HA structure up to collapse (Le Geros, Taheri, Quirolgico & Le Geros, 1980). In particular, numerous attempts have been made to incorporate magnesium into the HA structure, due

to its biological relevance. However, Mg^{2+} ions seem to be strongly rejected from the apatite lattice and their incorporation, if at all, is very limited (Thewlis, Glock & Murray, 1939; Carlstrom, 1955; Trautz, 1955; Klement & Haselbeck 1965; Kreidler & Hummel, 1970; Neuman & Mulryan, 1971; Simpson, 1972; Le Geros, 1984; Baravelli, Bigi, Foresti, Ripamonti & Roveri 1984).

The results of a structural and chemical characterization of apatites prepared from solutions in the presence of different amounts of magnesium indicate that the reduction of HA crystallite sizes is also great for very low magnesium content and increases on increasing magnesium concentration up to 35 atom-% when HA crystal growth is completely hindered (Bigi *et al.*, 1993). Furthermore, magnesium promotes the thermal conversion of HA into β-TCP, where it can partially replace calcium (Bigi *et al.*, 1988; Bigi *et al.*, 1992; Bigi *et al.*, 1993). The modifications of the values of the HA lattice constants induced by ionic substitution are generally in agreement with the difference in ionic radii between calcium and substituent ions (Heijligers, Driessens & Verbeck, 1979; Bigi, Gazzano, Ripamonti, Foresti & Roveri 1986; Bigi *et al.*, 1989; Bigi *et al.*, 1991). The poor resolution of the X-ray pattern of the apatitic phase synthesized in the presence of magnesium prevents an accurate determination of the lattice constant values and therefore does not allow to estabilish the extent of magnesium substitution for calcium (Bigi *et al.*, 1993).

X-ray powder profile fitting structure refinements using the Rietveld method have proved to be a powerful tool in detecting cationic substitution in the HA structure, even when the extent of cationic substitution is very low (Bigi *et al.*, 1989; DeBoer, Sakthivel, Cagle & Young, 1991).

Preliminary results of a Rietveld refinement of magnesium-substituted HA carried out using a limited 2θ range of diffraction data indicate that just a small amount of magnesium can be incorporated into the crystal lattice of HA (Bigi *et al.*, 1993).*

However, due to the low magnesium content in HA structure and to the small differences in the scattering factors between magnesium and calcium, the localization

---

* The numbered intensity of each measured point on the profile has been deposited with the IUCr (Reference: NA0066). Copies may be obtained through The Managing Editor, International Union of Crystallography, 5 Abbey Square, Chester CH1 2HU, England.

of magnesium in HA structure, which represents an extreme case of the application of the Rietveld method, requires a more accurate analysis using a wider 2θ range. Therefore, we have used different refinement procedures to carry out Rietveld structure refinements of hydroxylapatite samples prepared from solutions in the presence of 10, 15, 25 and 30 Mg-atom-%. For comparison, magnesium-free hydroxylapatite was refined using the same procedures.

The results substantiate a model for substitution of magnesium for calcium only at one of the two crystallographically independent metal sites.

2. Experimental

Hydroxylapatites at different magnesium contents were synthesized by adding calcium nitrate and magnesium nitrate solutions to ammonium dihydrogen phosphate solution with stirring in a N_2 atmosphere (Bigi *et al.*, 1993). The structure refinements were carried out on hydroxylapatite and on samples prepared in the presence of 10, 15, 25 and 30 Mg-atom-% (with respect to the total no. of metal atoms) in solution; the samples are named HA, Mg10, Mg15, Mg25 and Mg30. Magnesium and calcium content in the four magnesium-substituted samples was determined by atomic absorption spectrometry. Magnesium content incorporated in the solids was found to be 4.9, 14.1, 20.4 and 30.6 atom-%, respectively.

Powder X-ray diffraction analysis, for magnesium-substituted samples, was carried out using two independent sets of intensity data collected using a conventional source. The first set was collected with a Philips PW1050/81 diffractometer controlled by a PW1710 unit and equipped with a proportional counter; the second data set was obtained from a Rigaku DMAX-B diffractometer controlled by a MCD-2 unit and equipped with a scintillation counter. The results of the refinements do not show any appreciable variation as a function of the different sets of intensity data. Herein we report only the analysis carried out with the data from the Rigaku diffractometer. Data collection details are reported in Table 1. HA data were collected later, according to a referee's suggestion, using a Philips PW1050/81 diffractometer equipped with a graphite monochromator in the diffracted beam.

3. Structural analysis

The Rietveld refinements were performed using the atomic position set and the space group of the HA structure $P6_3/m$, no. 176 (Kay, Young, & Posner, 1964). The scattering factors for the Ca^{2+}, Mg^{2+} and O^- ions and the P atom were used (*International Tables for X-ray Crystallography*, 1974, Vol. IV).

The computer program *PREFIN* (Immirzi, 1980), improved for the possibility to refine the mean crystallite

Table 1. *Experimental details of X-ray powder profile data collection*

Radiation	Cu $K\alpha$ Ni-filtered (40 kV, 30 mA)*
	$\lambda_1 = 1.54051$, $\lambda_2 = 1.54433$ Å
Divergence slit (°)	0.5
Receiving slit (mm)	0.15
Scattering slit (°)	0.5
Step width (°)	0.03 (2θ)
Count time	20 s each step
2θ range (°)	15–135 (2θ) equivalent to 4000 steps
Temperature	Room temperature

* The data of the HA sample were collected with a graphite monochromator in the diffracted beam (see text).

size parallel to the crystallographic axes (Millini, Perego & Brückner, 1991), was employed. It is well known that HA crystals exhibit a preferential growth parallel to the c axis (Asada, Miura, Osaka, Oukami & Nakamura, 1988), therefore, a program that takes into account crystallite size anisotropy is the most suitable. The data were processed after correction for air scattering.

Rietveld refinement was carried out for all the samples HA, Mg10, Mg15, Mg25 and Mg30. First, the scale factor and background were refined. The background was approximated by a segmented line where only the height of the nodes was refined, while their positions on the 2θ scale were arbitrarily fixed.

The shape of the calculated background for the samples Mg10, Mg15, Mg25 and Mg30 indicates the presence of an amorphous component. Thus, for these samples the refinement was also carried out with the background modelled as a straight line with a superimposed Pearson VII-shaped curve. The bell height, the exponent of the Pearson VII curve, FWHM and the integrated intensity were refinable parameters, while the bell was assumed to be centred at a fixed value of 2θ.

At this point the pattern (peak widths and their dependence on 2θ, true 2θ zero, preferred orientation parameter, Pearson VII exponent) and structural parameters were also allowed to vary, but the individual isotropic atomic displacement parameters (a.d.p.) and the occupancy factors were held fixed, respectively, at the B_{eq} values obtained from the single-crystal structure determination (Kay, Young & Posner, 1964) and at the values corresponding to full occupied sites. Since no significant variation of the atomic positions was observed, they were held fixed during the following refinements in which successively the occupancy factors of the calcium ions were also allowed to vary. At this stage no significant occupancy factor variations were found for the samples HA and Mg10, while for the samples Mg15, Mg 25 and Mg 30 the Ca(2) occupancy factor appeared decreased and Ca(1) slightly increased. We interpreted this finding as evidence that in these samples magnesium substitutes only into Ca(2) sites. Therefore, the refinement proceeded by allowing a simultaneous presence of calcium and magnesium at the $6(h)$ site [site (2)]. Sites (2) were imposed to be fully

Table 2. *Refined structural parameters and agreement index R_{wp} for four different procedures*

A fixed isotropic B_{eq},* background as segmented line; *B* fixed isotropic B_{eq},* amorphous component as Pearson VII curve; *C* refined B_{iso},† background as segmented line; *D* refined B_{iso},† amorphous component as Pearson VII curve.

	Sample	$a = b$ (Å)	c (Å)	V (Å³)	OF (1)‡	OF (2)‡	Mg atom %§	Am (%)¶	$E_1 = E_2$ (Å)	E_3 (Å)	R_{wp}%**
A	HA	9.421 (2)	6.882 (3)	529.0 (4)	0.342 (3)	0.502 (2)	—		210 (2)	472 (12)	12.0
	Mg10	9.417 (2)	6.859 (3)	526.8 (4)	0.340 (2)	0.495 (3)	0.6 (3)		85.8 (5)	157 (2)	6.7
	Mg15	9.422 (3)	6.834 (5)	525.4 (7)	0.339 (1)	0.468 (3)	3.8 (3)		66.7 (5)	207 (3)	6.2
	Mg25	9.435 (4)	6.808 (6)	524 (8)	0.336 (2)	0.432 (5)	8.2 (6)		49.9 (5)	64 (1)	7.2
	Mg30	9.459 (5)	6.801 (9)	527 (1)	0.342 (2)	0.397 (5)	12.4 (6)		35.8 (4)	40.9 (5)	5.8
B	Mg10	9.416 (2)	6.858 (4)	526.6 (5)	0.345 (1)	0.487 (4)	1.6 (5)	8.6 (6)	89.3 (6)	135 (2)	8.7
	Mg15	9.418 (2)	6.833 (3)	524.9 (5)	0.342 (2)	0.452 (3)	5.8 (4)	7.0 (4)	64.3 (5)	218 (3)	7.2
	Mg25	9.432 (3)	6.806 (6)	524.4 (8)	0.337 (2)	0.442 (5)	7.0 (6)	7.9 (6)	47.8 (4)	60.1 (8)	8.0
	Mg30	9.459 (5)	6.800 (8)	527 (1)	0.338 (2)	0.433 (6)	8.0 (7)	8.6 (7)	36.5 (4)	40.0 (6)	7.1
C	HA	9.423 (2)	6.882 (3)	529.2 (4)	0.338 (1)	0.500 (1)	—		187 (2)	569 (9)	8.0
	Mg10	9.417 (2)	6.859 (3)	526.8 (4)	0.339 (2)	0.494 (3)	0.7 (3)		86.5 (5)	134 (8)	6.9
	Mg15	9.422 (2)	6.833 (3)	525.3 (5)	0.333 (2)	0.468 (4)	3.8 (4)		62.3 (5)	235 (8)	5.7
	Mg25	9.437 (4)	6.808 (6)	525.1 (8)	0.330 (2)	0.424 (5)	9.1 (6)		51.3 (4)	62.1 (8)	6.7
	Mg30	9.459 (6)	6.804 (9)	527 (2)	0.328 (2)	0.397 (4)	12.4 (5)		36.2 (3)	41.5 (5)	5.2
D	Mg10	9.415 (2)	6.858 (3)	526.5 (4)	0.350 (3)	0.488 (4)	1.4 (4)	8.7 (5)	90.8 (6)	141 (2)	8.5
	Mg15	9.425 (4)	6.834 (5)	525.7 (6)	0.341 (2)	0.450 (4)	6.0 (6)	6.1 (3)	62.9 (5)	227 (4)	7.4
	Mg25	9.435 (4)	6.808 (6)	524.8 (8)	0.340 (2)	0.445 (4)	6.6 (5)	8.2 (6)	49.2 (4)	63.5 (8)	7.6
	Mg30	9.462 (6)	6.803 (9)	527 (1)	0.339 (2)	0.442 (6)	7.0 (8)	8.9 (8)	35.7 (4)	41.2 (6)	6.8

* The following B_{eq} (Å²) values were used (calculated from Kay, Young & Posner, 1964): $O(1) = 0.70$; $O(2) = 0.96$; $O(3) = 1.19$; $P = 0.48$; $Ca(1) = 0.81$; $Ca(2) = 0.70$; $O(H) = 1.26$; $H = 3.3$. † Refined B_{iso} are reported as supplementary material. ‡ Occupancy factors for Ca atoms. In stoichiometric calcium apatite the values corresponding to sites completely filled by calcium are $OF(1) = 0.3333$; $OF(2) = 0.5000$. § Percentage calculated from the formula: $\{[0.5\text{-}OF(2)]/0.8333\} \times 100$. ¶ Amorphous phase content percentage. ** $R_{wp} = \{\sum_i w_i (y_i(\text{obs}) - y_i(\text{calc}))_i^2 / [\sum_i w_i (y_i(\text{obs}))^2]\}^{1/2}$.

Table 3. *Refined non-structural parameters obtained using a.d.p. expressed as B_{eq} and fitting amorphous component as Pearson VII curve*

	Mg10	Mg15	Mg25	Mg30
2θ zero correction (°)	0.027 (3)	0.011 (4)	0.023 (5)	0.006 (7)
Scale factor	0.01327 (7)	0.01403 (8)	0.01339 (7)	0.01529 (8)
Profile function parameters*				
U	0.250 (1)	−0.014 (3)	0.0 (2)	0.0 (3)
V	0.123 (1)	0.675 (2)	0.0 (1)	0.0 (2)
W	0.624 (3)	0.655 (4)	14.09 (5)	13.4 (3)
m†	1.12 (1)	0.959 (3)	0.972 (2)	0.853 (7)
Asymmetry parameters‡	38.1 (8)	87.4 (1)	93.9 (2)	93.9 (2)
Background intensities at the nodes of the semented line (counts)				
$2\theta(°) = 14.99$	439 (2)	449 (2)	461 (2)	447 (2)
135.00	439 (2)	449 (2)	461 (2)	447 (2)
Amorphous phase integral§ (counts deg⁻¹ × 10⁻³)	2.38 (4)	2.03 (4)	2.0 (1)	2.4 (2)

* According to the relation $H_k^2 = U \tan^2 \theta_k + V \tan \theta_k + W$, m is the exponent in the Pearson VII profile function $f(z) = (C/H_k)[1 + 4(2^{1/m} - 1)z^2]^{-m}$ with $z = (2\theta_i - 2\theta_k)/H_k$. The contemporary refinement of U, V and W and E_1, E_2 and E_3 was not possible for the high correlation. † An angular limit of influence equal to $5 \times$ FWHM was used for each peak. ‡ Peak asymmetry is described adopting two half-peak functions with different HWHM, H_k' and H_k'' with $H_k' - H_k'' = 2A(2\theta)^{-2}$ (see Millini, Perego & Brückner, 1991, for details). § Amorphous phase is represented by one Pearson VII curve superimposed onto the background line (centre at $2\theta = 39°$, FWHM=20°, $m' = 3$).

occupied by magnesium and calcium, while no constraint was imposed on the overall magnesium content. In contrast, with a substantially good overall agreement, the calculated FWHM values of the (002) and (004) reflections were appreciably wider than the experimental values. No improvement was obtained by refining the preferred orientation parameter. The refinement of the mean crystallite sizes parallel to the crystallographic axes, carried out imposing the same dimension along a and b in order to maintain the hexagonal symmetry, led to a clear decrease of R_{wp} from 13 to $\sim$ 8%.

In Fig. 1 we compare the experimental pattern and the profiles calculated taking or not taking into account the crystallite size anisotropy to emphasize how this factor can contribute to a successful refinement.
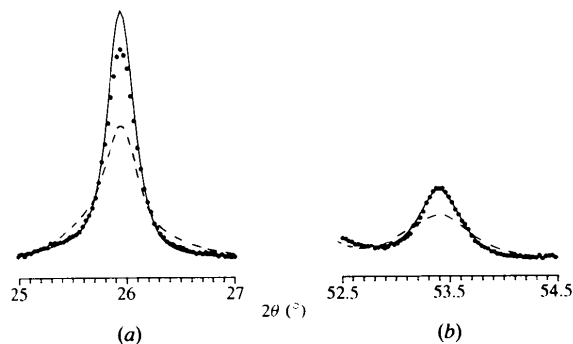

Fig. 1. Profiles of the (*a*) 002 and (*b*) 004 reflections. The points are the experimental values, the full line the profile calculated taking into account the crystal size anisotropy and the dashed line that calculated using isotropic crystallite size.

In order to test the influence of the fixed B_{eq} used in the refinement procedure, we carried out further cycles where the a.d.p. were also allowed to vary. Due to the strong correlation between a.d.p. and occupancy factors, further refinements were carried out by fixing alternatively the isotropic a.d.p. and the occupancy factors. The a.d.p. values for metal ions at both 4(f) and 6(h) sites were imposed to be identical.

Refined structural parameters obtained from the four different refinement procedures are reported in Table 2, together with the agreement index R_{wp}. To show typical data, observed and calculated patterns from the refinements carried out with the inclusion of a 'bell-shaped' curve for the amorphous component and with fixed isotropic B_{eq} are compared in Fig. 2.

Refined non-structural parameters obtained from this refinement are reported in Table 3.

4. Discussion

The results of the powder fitting structure refinements of magnesium-substituted samples indicate that just a limited amount of magnesium is incorporated into the hydroxylapatite lattice. There is no appreciable evidence of magnesium substitution in the sample Mg10, while in the samples Mg15, Mg25 and Mg30 the degree of magnesium occupancy reaches a maximum value of $\sim 12\%$. No significant variation of the calcium occupancy factors, with respect to the theoretical values of the space group, was observed for HA using the same
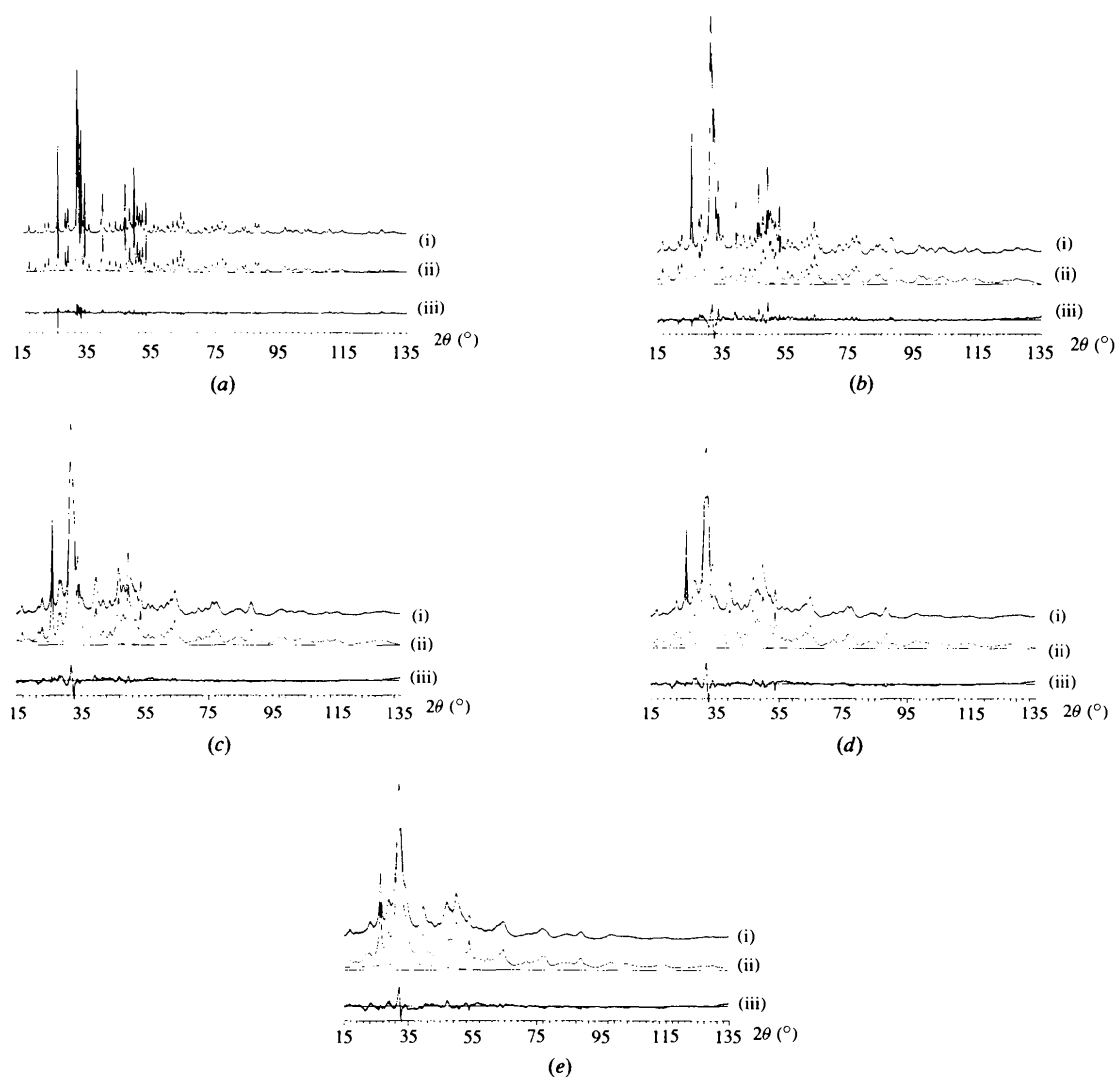

Fig. 2. Comparison between (i) the observed, (ii) calculated and (iii) difference powder diffraction patterns of (a) HA, (b) Mg10, (c) Mg15, (d) Mg25 and (e) Mg30 samples. The full line represents the calculated background, the dashed line the amorphous contribution.

2θ range of diffraction data and the same refinement strategies. This supports the reliability of the results on magnesium structural incorporation, which represents the main aim of our study. The limited magnesium incorporation into the HA structure is in agreement with the principle that ions significantly larger than Ca^{2+} can be substituted, but smaller ions do not tend to substitute extensively for calcium (Lang, 1981). However, theoretical considerations of magnesium incorporation in the apatite lattice suggest that the substitution of Mg for Ca cannot be excluded on the basis of ionic radii, although magnesium represents a borderline case (Terpstra & Driessens, 1986).

Magnesium substitution for calcium into the HA structure induces a slight contraction of the unit cell, as expected for a low level of magnesium incorporation. On the contrary, Mg30 exhibits a slight enlargement of the HA unit cell. Probably the lattice parameters in this case exhibit underestimated e.s.d. values, because of the broadening of the peak profiles. Thus, it seems that no meaning can be attached to the variation of the cell parameters with the magnesium content.

In spite of the limited magnesium incorporation in the HA structure, the analytical results indicate a significantly higher magnesium presence in the solid phase. The results of the refinements indicate the presence of an almost constant amount of amorphous component which reaches a maximum value of $\sim$ 9%. The amorphous phase could be a phosphate rich in magnesium, which, together with that possibly located on the crystallite surface, could account for the discrepancy between magnesium content in the solid phase and in the HA structure.

The broadening of the diffraction peaks increases on increasing the magnesium content until the apatite crystallization is completely hindered. This can be due to the increase in the lattice defects and/or to the decrease of crystallite sizes. The program *PREFIN* allows the refinement of the average crystallite sizes along the crystallographic axes (*E* parameters), but it does not take into account the lattice strain effects. Furthermore, the *E* values are strongly correlated with the profile function parameters. Thus, it is difficult to attach a physical meaning to the refined *E* values. However, the sound decrease of the mean crystallite sizes confirmed by the results of four different refinement procedures, on increasing magnesium concentration, suggests that the general trend of the *E* values is real. Furthermore, the shape of the crystallites changes so that the dimension along the *c* direction becomes very close to that along the orthogonal.

From the metal-site occupancy factors it appears evident that magnesium incorporated into the HA structure substitutes essentially in the Ca(2) sites. This preference may be explained on the basis of the different metal–oxygen interactions and of the different geome-

tries of the two distinct metal sites in the HA structure, shown in Fig. 3. In site (1) six oxygens arranged in a distorted trigonal prism are bonded to the central atom with distances shorter than 2.46 Å (average Ca—O distance: 2.429 Å). The other three O atoms are at a distance of 2.805 Å. In site (2) the metal is strongly coordinated by four O atoms arranged in a distorted tetrahedron (average Ca—O distance: 2.357 Å); two other O(3) atoms at the same edge are at 2.512 Å and a further O(1) atom is at 2.705 Å (Kay, Young & Posner 1964). The shorter metal–oxygen distance in site (2) seems more suitable to support magnesium substitution for calcium. However, metal–oxygen distances must not be the main factor in dictating cationic site preference, since also cations greater than Ca^{2+}, such as Pb^{2+} and Sb^{3+}, display a preference for site (2) (Bigi *et al.*, 1989; DeBoer, Sakthivel, Cagle & Young, 1991). This behaviour can be accounted for by the geometry of the anion coordination of Ca(2), which is 'ill-defined' and therefore more suitable to support cationic substitution for calcium.

The four different refinement approaches brought similar and satisfactory R_{wp} values and allowed to appreciate the influence of some parameters on the refinements results. The effect of the assumption made in the refinement cycles of magnesium-substituted samples in which B_{iso} were used [*i.e.* site (1) a.d.p. = site (2) a.d.p.] does not seem to be very important. In fact, the occupancy factors are very similar to those obtained in the refinements carried out using different B_{eq} [*i.e.* site (1) a.d.p. = 0.81 Å², site (2) a.d.p. = 0.70 Å²].

More significant seems to be the estimate of the amorphous and background diffusion profiles, as can be inferred from the data reported in Table 2. However, the results of the different refinement approaches point to the same conclusions: magnesium is incorporated into the HA structure and is preferentially located in site (2). On

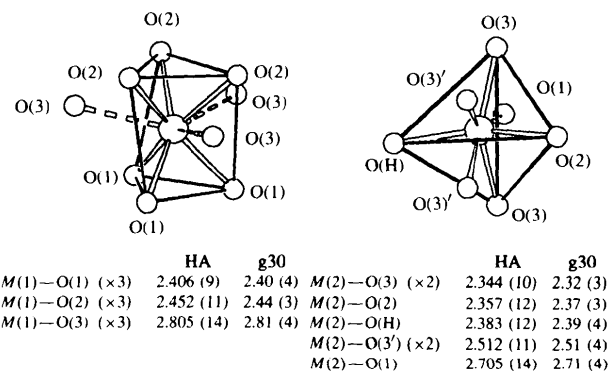|	HA	g30		HA	g30
$M(1)$—$O(1)$ ($\times 3$)	2.406 (9)	2.40 (4)	$M(2)$—$O(3)$ ($\times 2$)	2.344 (10)	2.32 (3)
$M(1)$—$O(2)$ ($\times 3$)	2.452 (11)	2.44 (3)	$M(2)$—$O(2)$	2.357 (12)	2.37 (3)
$M(1)$—$O(3)$ ($\times 3$)	2.805 (14)	2.81 (4)	$M(2)$—$O(H)$	2.383 (12)	2.39 (4)
			$M(2)$—$O(3')$ ($\times 2$)	2.512 (11)	2.51 (4)
			$M(2)$—$O(1)$	2.705 (14)	2.71 (4)

Fig. 3. A view of the environments of the two independent Ca atoms with the HA interatomic distances (Å). The smaller values of some of the Mg30 interatomic distances, reported for comparison, reflect the contraction of the *c* axis. The atomic coordinates and labelling are taken from Kay, Young & Posner (1964).

the other hand, the amount of magnesium incorporation appears to be more affected by the refinement procedure. However, the trend clearly indicates an increase of magnesium incorporation in the structure on increasing magnesium content in the solid phase up to a maximum value ranging from *ca* 8 to 12%.

References

Asada, M., Miura, Y., Osaka, A., Oukami, K. & Nakamura, S. (1988). *J. Mater. Sci.* **23**, 3202–3205.

Baravelli, S., Bigi, A., Foresti, E., Ripamonti, A. & Roveri, N. (1984). *J. Inorg. Biochem.* **20**, 1–12.

Bigi, A., Compostella, L., Fichera, A. M., Foresti, E., Gazzano, M., Ripamonti, A. & Roveri, N. (1988). *J. Inorg. Biochem.* **34**, 75–82.

Bigi, A., Falini, G., Foresti, E., Gazzano, M., Ripamonti, A. & Roveri, N. (1993). *J. Inorg. Biochem.* **49**, 69–78.

Bigi, A., Foresti, E., Gregorini, R., Ripamonti, A., Roveri, N. & Shah, J. S. (1992). *Calcif. Tissue Int.* **50**, 439–444.

Bigi, A., Gandolfi, M., Gazzano, M., Ripamonti, A., Roveri, N. & Thomas, A. (1991). *J. Chem. Soc. Dalton Trans.* pp. 2883–2886.

Bigi, A., Gazzano, M., Ripamonti, A., Foresti, E. & Roveri, N. (1986). *J. Chem. Soc. Dalton Trans.* pp. 241–244.

Bigi, A., Ripamonti, A., Brückner, S., Gazzano, M., Roveri, N. & Thomas, S. A. (1989). *Acta Cryst.* B**45**, 247–251.

Carlstrom, D. (1955). *Acta Radiol.* Suppl. Sverige **121**, 1.

DeBoer, B. G., Sakthivel, A., Cagle, J. R. & Young, R. A. (1991). *Acta Cryst.* B**47**, 683–692.

Heijligers, H. M., Driessens, F. C. M. & Verbeck, R. M. H. (1979). *Calcif. Tissue Int.* **29**, 127–131.

Kay, M. I., Young, R. A. & Posner, A. S. (1964). *Nature*, **204**, 1050–1052.

Klement, R. & Haselbeck, H. (1965). *Z. Anorg. Chem.* **336**, 113–128.

Kreidler, E. R. & Hummel, F. A. (1970). *Am. Miner.* **55**, 170–184 (abstr.).

Immirzi, A. (1980). *Acta Cryst.* B**36**, 2378–2385.

Lang, J. (1981). *Bull. Soc. Sci. Bretagne*, **53**, 95–124.

Le Geros, R. Z. (1984). *Tooth Enamel. Proc. Int. Symp. Compos., Prop. Fundam. Struct. Tooth Enamel*, edited by R. W. Fearnhead & S. Suga, Vol. IV, pp. 32–36. Amsterdam: Elsevier Science Publishers.

Le Geros, R. Z. & Le Geros, J. P. (1984). *Phosphate Minerals*, edited by J. O. Nriagu & P. Moore, pp. 351–385. New York: Springer-Verlag.

Le Geros, R. Z., Taheri, M. M., Quirolgico, G. B. & Le Geros, J. P. (1980). *Proc. 2nd Int. Congress on Phosphorus Compounds*, pp. 89–103. Boston.

Millini, R., Perego, G. & Brückner, S. (1991). *Mater. Sci. Forum*, **79–82**, 239–244.

Nancollas, G. H. (1982). *Biological Mineralization and Demineralization*, edited by G. H. Nancollas, pp. 79–99, Dahlem Konferenzen. Berlin: Springer-Verlag.

Neuman, W. F. & Mulryan, B. J. (1971). *Calcif. Tissue Res.* **7**, 133–138.

Simpson, D. R. (1972). *Clin. Orthop.* **86**, 260–286.

Terpstra, R. A. & Driessens, F. C. M. (1986). *Calcif. Tissue Int.* **39**, 348–354.

Thewlis, J., Glock, G. E. & Murray, M. M. (1939). *Trans. Faraday Soc.* **35**, 358–363.

Trautz, O. R. (1955). *Ann. N. Y. Acad. Sci.* **60**, 696–712.